

Nucleus-Nucleus Long-Range Interaction Potential in Elastic Scattering*†

J. S. McINTOSH,‡ S. C. PARK,§ AND G. H. RAWITSCHER

Department of Physics, Yale University, New Haven, Connecticut

(Received 16 January 1964)

Differential cross sections are calculated for the elastic scattering of heavy nuclei by heavy nuclei and the results are compared with experiment. The long-range part of the nucleus-nucleus interaction is assumed to be representable by a two-body potential, and the attempt is made to calculate the latter in terms of the experimentally determined nucleon-nucleus optical-model potential extrapolated to negative energies and an adjustable reduced width parameter which determines the probability of finding individual nucleons at the surface of each nucleus. The short-range part of the nucleus-nucleus interaction is represented schematically by a complex potential or an ingoing wave boundary condition, the justification for which as a representation of the optical-model potential is given below. Reasonable agreement with experiment is obtained for the experimental data considered, i.e., those for $C^{12}-O^{16}$, $N^{14}-N^{14}$, and $C^{12}-N^{14}$ if the average-reduced-width parameter equal to about one-fifth the corresponding single-particle value is employed.

I. INTRODUCTION

THE inherent complexities in the interaction of one heavy nucleus with another due to the many particles involved, as well as lack of precise knowledge of the interparticle forces present formidable obstacles to the complete theoretical investigation of the elastic scattering.

Various simplified models have been employed in the literature. In the first attempt, Reynolds and Zucker¹ analyzed their $N^{14}-N^{14}$ data in terms of the so-called "sharp cutoff model" which had been developed by Blair² for the analysis of α -particle scattering. This procedure, recognizing that a major part of the scattering arises from the "shadow scattering" caused by strong absorption for close approach of the heavy nuclei, assumes that in the partial-wave expansion of the Coulomb amplitude, all partial waves from $L=0$ up to a critical value L_{\max} are completely absorbed and those partial waves corresponding to larger L are unmodified. The distance of closest approach for a classical particle of angular momentum $L_{\max}\hbar$ is then assumed to determine the nuclear radius. Reynolds and Zucker's analysis resulted in a good representation of experimental data employing a nuclear radius of $1.66 \times A^{1/3}$ F, somewhat larger than might have been expected. Porter³ analyzed the $N^{14}-N^{14}$ scattering by means of an optical potential with the shape suggested by Woods and Saxon for nucleon-nucleus scattering, the parameters being adjusted to fit experiment. A similar analysis of their extensive $C^{12}-N^{14}$ scattering data has recently been carried out by Kuehner and Almqvist.⁴

* Supported by U. S. Atomic Energy Commission, U. S. Army Research Office (Durham) and the U. S. Air Force Office of Scientific Research.

† Part of the work here presented is part of work for a dissertation of one of the authors (S. C. P.).

‡ Present address: Wesleyan University, Middletown, Connecticut.

§ Present address: Florida State University, Tallahassee, Florida.

¹ H. L. Reynolds and A. Zucker, *Phys. Rev.* **102**, 1378 (1956).

² J. S. Blair, *Phys. Rev.* **95**, 1218 (1954).

³ C. E. Porter, *Phys. Rev.* **112**, 1722 (1958).

⁴ J. A. Kuehner and E. Almqvist, *Proceedings of the Third Conference on Reactions Between Complex Nuclei*, edited by A.

In the work quoted above as well as in other available treatments the nucleus-nucleus interaction is considered almost entirely phenomenologically. The elastic scattering data combined with other evidence concerning the approximate magnitude of nuclear radii form the only guides in arriving at the phenomenological models. In the work reported below an attempt is made to correlate the nucleus-nucleus elastic scattering data with nucleon-nucleus elastic scattering information by deriving from the latter an effective long-range nucleus-nucleus interaction potential and to employ this potential as a guide in the nucleus-nucleus scattering analysis. The short-range nucleus-nucleus interaction is, on the other hand, treated phenomenologically. In view of the desirability of comparing any theoretical estimate of long-range nucleus-nucleus interactions as directly as possible with corresponding elastic scattering data one of the main objectives of the present work was to investigate how much information on the long-range part of the nucleus-nucleus interaction can be obtained from the elastic scattering and to what extent the unknown short-range part has to be brought in.

A long-range two-body interaction potential is derived making use of the experimental nucleon-nucleus separation energies and the nucleon-nucleus elastic scattering optical-model potential determined from the elastic scattering experiments of protons on various nuclei.⁵ For each nucleus there is introduced into the calculation a free parameter which is related to the average value of one of the bound protons' or neutrons' wave functions at the nuclear surface. The parameter is adjusted to give the best fit to the experimental nucleus-nucleus elastic scattering angular distribution. This adjustment amounts to a determination of the average reduced width of the transferred particles in the emitting and receiving nuclei. It would be unrealistic to suppose that a two-body potential could really be taken seriously for separation distances corre-

Ghiorso, R. M. Diamond, and H. E. Conzett (University of California Press, Berkeley, California, 1963).

⁵ The authors wish to thank Professor G. Breit for suggesting the approach outlined below.

sponding to overlap of the nuclear matter. For such distances, however, the interaction of the two nuclei is dominated by the strong absorption and if it is assumed that this part of the interaction can be represented schematically by complex two-body potentials or boundary conditions, then it can be shown under certain conditions that the resulting cross section is very insensitive to the assumed form of that part of the interaction.

In Sec. II are outlined the theory and assumptions involved in the calculation of the potential tails for the $N^{14}-N^{14}$, $N^{14}-C^{12}$, and $C^{12}-O^{16}$ systems; in Sec. III a comparison is made with experiment.

A list of the most frequently used symbols is given below.

\mathcal{F}_L	nucleus-nucleus radial wave functions, as defined in Eq. (16).
l, L	nucleon orbital angular momenta relative to emitter and receiver nuclei, respectively.
R	center-to-center distance of the two complex nuclei.
$\Delta E(R)$	change in the energy eigenvalue of the two complex nuclei which vanishes as $R \rightarrow \infty$.
$\Psi^{(0)}, \Psi$	undistorted and distorted many-body wave functions describing the two-nucleus system.
$\psi^{(0)}, \psi$	undistorted and distorted single-nucleon wave functions.
$c_s^{(0)}, c_p^{(0)}$	nucleon wave function normalization parameters, defined in Eq. (3); having dimensions of $(\text{length})^{-3/2}$. Subscripts s and p denote angular momenta 0 and 1 with respect to the emitter nucleus.
$\alpha_s^{(0)}, \alpha_p^{(0)}$	$= (2m E_{s,p}^{(0)} / \hbar^2)^{1/2}$.
m, μ	the mass of a nucleon, reduced mass of the nucleus-nucleus system, respectively.
A_L^s, A_L^p	parameters describing distortion of nucleon wave functions introduced in Eq. (5).
V, \mathcal{U}, V^m	nucleon-nucleus, nucleus-nucleus, and auxiliary shell-model potentials as defined in Eqs. (8a), (15), and (19).
V_0, R_0, a	nucleon-nucleus optical parameters obtained from experimental elastic scattering data.
γ_L^l	homogeneous logarithmic derivative of radial wave function defined below Eq. (9).
$\delta E_s, \delta E_p$	single nucleon energy shifts of individual s and p nucleons in presence of second nucleus.
$K_L = a_L + ib_L$	nuclear part of complex nucleus-nucleus phase shift.
r, r'	nucleon radial coordinate relative to the center of the emitter and receiver nuclei.
ρ, ρ_{sb}	reduced width and single-body reduced-width parameters defined in Eq. (18). Their units are $(\text{length})^3$.

II. CALCULATIONS

The basic ideas for the calculation⁶ of the long-range potential tail, suggested to the authors by Professor G. Breit, are as follows. In an adiabatic description of the process, when two complex nuclei are so far apart that the tails of the individual nucleon wave functions from one nucleus penetrate the other only slightly, a small change in the total energy of the system takes place, which according to Born and Oppenheimer may be considered as a contribution to the potential energy between the two nuclei. The change ΔE , in the total internal energy of the system, from that at infinite nuclear separation is then given by⁷

$$\Delta E = (\Psi^{(0)}, H' \Psi) / (\Psi^{(0)}, \Psi), \quad (1)$$

where H' is the many-body interaction energy between the two nuclei and Ψ and $\Psi^{(0)}$ are the exact many-body distorted and undistorted wave functions of the system respectively. This total change in the energy is a function of the internuclear separation R . In the adiabatic approximation the motions of the individual nucleons are supposed to be fast compared to the motion of the centers of the two nuclei, and the problem is thereby reduced to the consideration of the motion of the nucleons about two fixed-force centers. For each internuclear separation R , ΔE is calculated by means of Eq. (1) and the resulting function of R is taken as a nucleus-nucleus potential energy function in a two-body Schrödinger equation in much the same spirit as that of the Born-Oppenheimer approximation. Since H' is the interaction between the nucleons of one nucleus with those of the other, the integral in the numerator of Eq. (1) involves the tail of the nuclear wave function of the first nucleus in the region where it overlaps the second, and vice versa. For large internuclear separations and large distances from the center of a given nucleus, the density of nuclear matter is small and consequently the nuclear wave function in this part of space is approximated by the product of the tails of the individual nucleon wave functions, the coupling between them being considered to be negligibly small. On account of the general connection between phase shifts and energy⁷ the contribution of the many body H' to ΔE arising from each nucleon tail is then equal to that produced by an equivalent nucleon-nucleus optical potential provided the latter may be suitably extrapolated to negative energies. For positive nucleon energies the *nucleon-nucleus* optical potential $V(r)$ produces the same phase shifts as H' , and this (energy-dependent) potential has been determined from the

⁶ *Proceedings of the Second Conference on Reactions Between Complex Nuclei, Gallinburg, Tennessee, 1960*, edited by A. Zucker, F. T. Howard, and E. C. Halbert (John Wiley & Sons, Inc., New York, 1960), p. 127; *Proceedings of the Third Conference on Reactions Between Complex Nuclei*, edited by A. Ghiorso, R. M. Diamond, and H. E. Conzett (University of California Press, Berkeley, California, 1963); *Bull. Am. Phys. Soc.* 8, 61 (1963).

⁷ G. Breit, *Rev. Mod. Phys.* 23, 238 (1951).

scattering data by various authors⁸ with varying degrees of sophistication, the more variable parameters employed the better the reproduction of the data. All of them "mock up" the removal of particles from the elastic scattering beam (inelastic scattering, reactions) by a complex part to the optical potential which goes to zero as the energy goes to zero. In the present work the nucleon tails correspond to bound (*negative energy*) nucleons and the energy-dependent parameters of the optical potential are extrapolated to negative energies *linearly*. There is of course some question of the validity of this linear extrapolation.

Under the assumptions of the preceding paragraph, if the many-body wave function were normalized such that

$$(\Psi^{(0)}, \Psi^{(0)}) = 1$$

then with the neglect of the second order changes in the wave function tail of one nucleon in the vicinity of the receiver nucleus due to the presence of another nucleon wave function tail, the total ΔE splits up into

$$\Delta E = \sum_i \int \psi^{(0)*}(\mathbf{r}_i) V(|\mathbf{R} - \mathbf{r}_i|) \psi(\mathbf{r}_i) d\mathbf{r}_i \equiv \sum_i \delta E_i \quad (2)$$

since the V is nonzero only in this vicinity and the denominator of Eq. (1) is approximately unity, i.e.,

$$(\Psi^{(0)}, \Psi) = 1. \quad (2a)$$

In Eq. (2) $\psi^{(0)}(\mathbf{r}_i)$ and $\psi(\mathbf{r}_i)$ are, respectively, the undistorted and distorted nucleon wave functions from one of the nuclei and \mathbf{R} is the vector from the center of that nucleus to the center of the other nucleus, whose effect on each nucleon tail is replaced by the optical potential. Equation (2a) represents a further assumption in that this calculation is to be applied for inter-nuclear distances large enough so that the difference between the quantity which should have been in the denominator of Eq. (2),

$$(\psi^{(0)}, \psi)_{sb},$$

and the normalization integral

$$(\psi^{(0)}, \psi^{(0)})_{sb}$$

gives rise to a contribution in ΔE which is of higher order and can be neglected. The symbol ψ is used for the single-body wave function without spin, in contradistinction to the many-body Ψ of Eq. (1).

At large distances from one of the nuclei, the undistorted individual nucleon wave functions of nucleons emanating from that nucleus are denoted by $\psi_{l,m}^{(0)}$. Here $\hbar l$ denotes the angular momenta about that nucleus, and $\hbar m$ is the projection along the polar axis chosen to be in the \mathbf{R} direction. For $l=0$ and 1, respectively, the corresponding wave functions are given

outside the parent nucleus by

$$\begin{aligned} \psi_{0,0}^{(0)} &= c_s^{(0)} (1/\alpha_s^{(0)} r) \exp(-\alpha_s^{(0)} r) Y_{0,0}(\theta, \varphi), \\ \alpha_s^{(0)} &= (2m|E_s^{(0)}|/\hbar^2)^{1/2}, \\ \psi_{1,m}^{(0)} &= c_p^{(0)} [(1/\alpha_p^{(0)} r) + (1/\alpha_p^{(0)} r)^2] \\ &\quad \times \exp(-\alpha_p^{(0)} r) Y_{1,m}(\theta, \varphi), \\ \alpha_p^{(0)} &= (2m|E_p^{(0)}|/\hbar^2)^{1/2}, \end{aligned} \quad (3)$$

where $E_s^{(0)}$ and $E_p^{(0)}$ denote the unperturbed s and p state nucleon binding energies and the real constants $c_s^{(0)}$ and $c_p^{(0)}$ are determined by the values of the respective $\psi^{(0)}$'s at the nuclear surface. Higher angular momenta are not needed for the p -shell nuclei under consideration.

The s -wave function, $l=0$ for one nucleus, when expanded in terms of spherical harmonics centered on the nucleus is given by⁹

$$\begin{aligned} \psi_{0,0}^{(0)} &= c_s^{(0)} \sum_{L=0}^{\infty} \xi_L^s(\alpha_s^{(0)} R) \\ &\quad \times [I_{L+\frac{1}{2}}(\alpha_s^{(0)} r') / (\alpha_s^{(0)} r')^{1/2}] Y_{L,0}(\theta', \varphi') \quad (4a) \\ \text{with} \quad \xi_L^s(x) &\equiv (2L+1)^{1/2} K_{L+\frac{1}{2}}(x) / x^{1/2}, \end{aligned}$$

where the primed quantities refer to a frame of reference centered at the right nucleus and I_n and K_n are Bessel functions of imaginary argument where the notation agrees with that employed by Watson.⁹ A similar expression may be derived for the p -wave functions using the relations¹⁰

$$\begin{aligned} (\alpha)^{-3/2} (\partial/\partial x' \pm i\partial/\partial y') \\ \times [(r')^{-1/2} I_{L+\frac{1}{2}}(\alpha r') P_L(\cos\theta')] &= \frac{(4\pi)^{1/2} (\alpha r')^{-1/2}}{2L+1} \\ \times \left\{ \pm \left[\frac{(L+2)(L+1)}{2L+3} \right]^{1/2} Y_{L+1,\pm 1}(\theta', \varphi') I_{L+\frac{1}{2}}(\alpha r') \right. \\ &\quad \mp \left. \left[\frac{L(L-1)}{2L-1} \right]^{1/2} Y_{L-1,\pm 1}(\theta', \varphi') I_{L-\frac{1}{2}}(\alpha r') \right\}, \\ \alpha^{-3/2} \frac{\partial}{\partial z'} [(r')^{-1/2} I_{L+\frac{1}{2}}(\alpha r') P_L(\cos\theta')] &= \frac{(4\pi)^{1/2} (\alpha r')^{-1/2}}{2L+1} \\ \times \left\{ \frac{(L+1)}{(2L+3)^{1/2}} Y_{L+1,0}(\theta') I_{L+\frac{1}{2}}(\alpha r') \right. \\ &\quad \left. + \frac{L}{(2L-1)^{1/2}} Y_{L-1,0}(\theta') I_{L-\frac{1}{2}}(\alpha r') \right\}. \end{aligned}$$

When $\partial/\partial x' \pm i\partial/\partial y'$ and $\partial/\partial z'$ are applied to (4a), the

⁹ G. N. Watson, *Theory of Bessel Functions* (Cambridge University Press, Cambridge, England, 1952).

¹⁰ The authors are indebted to G. Breit for having pointed out to them the derivation which leads to Eqs. (4b).

⁸ The parameters used were those of Bjorklund (nucleon-nucleus optical-model potential) referred to in footnote 13.

following expressions result:

$$\psi_{1,m}^{(0)} = -3^{1/2} c_p^{(0)} \sum_{L=0}^{\infty} \xi_{L,p,m}(\alpha_p^{(0)} R) \times \left[\frac{I_{L+\frac{1}{2}}(\alpha_p^{(0)} r')}{(\alpha_p^{(0)} r')^{1/2}} \right] Y_{L,m}(\theta', \varphi'), \quad (4b)$$

where

$$\begin{aligned} \xi_{L,p,0}(x) &\equiv [(2L+1)x]^{-1/2} \\ &\quad \times [LK_{L-\frac{1}{2}}(x) + (L+1)K_{L+\frac{1}{2}}(x)], \\ \xi_{L,p,\pm 1}(x) &\equiv \pm [L(L+1)/(2L+1)x]^{1/2} \\ &\quad \times [K_{L-\frac{1}{2}}(x) - K_{L+\frac{1}{2}}(x)]. \end{aligned}$$

The distorted-wave functions $\psi_{L,m}$ are calculated on the assumption that under the physical conditions of large nuclear separation here considered, a region surrounding both nuclei exists within the nucleon-nucleus potentials are negligible. This region is denoted by III. The region surrounding the nucleus from which the tails of the single nucleon wave functions protrude is denoted by I and the region surrounding the "receiver" nucleus, outside of which the optical-model potential is negligible is denoted by II. The distorted-wave functions of nucleons extending from the surface of region I into region III are obtained subject to the conditions: (A) that in region II they satisfy the Schrödinger equation with optical potential V and energy approximated by the unperturbed energy E_0 , and (B) that in region III they be given by

$$\begin{aligned} \psi_{0,0} &= c_s \sum_{L=0}^{\infty} \xi_{L,s}(\alpha_s^{(0)} R) [\alpha_s^{(0)} r']^{-1/2} \\ &\quad \times [I_{L+\frac{1}{2}}(\alpha_s^{(0)} r') + A_L^s K_{L+\frac{1}{2}}(\alpha_s^{(0)} r')] Y_{L,0}(\theta' \varphi'), \end{aligned}$$

$$\begin{aligned} \psi_{1,m} &= -3^{1/2} c_p \sum_{L=0}^{\infty} \xi_{L,p,n}(\alpha_p^{(0)} R) [\alpha_p^{(0)} r']^{-1/2} \\ &\quad \times [I_{L+\frac{1}{2}}(\alpha_p^{(0)} r') + A_L^p K_{L+\frac{1}{2}}(\alpha_p^{(0)} r')] Y_{L,m}(\theta', \varphi'), \quad (5) \end{aligned}$$

where the coefficients A_L are calculated by matching the logarithmic derivatives of the distorted-wave functions in region II to those in region III.

The potential producing the distortion is that described in connection with Eq. (2). As described above the many-body interaction energy in region II is replaced by an (energy-dependent) complex optical-model potential for each nucleon defined so as to reproduce the observed nucleon-nucleus scattering for positive energies. The real part of this is linearly extrapolated to negative energies. The imaginary part of the nucleon-nucleus optical potential goes to zero at zero energy, but of course this does not mean that there is no absorption for the nucleus-nucleus system. Indeed it is expected that in the collision of two complex nuclei an increasingly large number of inelastic scattering and reaction channels are opened up as the bombardment

energy rises and that the resulting "shadow" scattering predominates, at least for the larger scattering angles. The success of the Blair procedure as employed by Reynolds and Zucker to give fair agreement with their $N^{14}-N^{14}$ scattering data bears out this contention. The nucleus-nucleus elastic channel absorption may be simulated in several ways, one of which consists in the introduction of an imaginary part to the potential energy, as is done in the nucleon-nucleus problem. An alternative to the use of imaginary potentials consists in imposing an ingoing wave boundary condition on each partial wave.¹¹ For certain complex optical-model potentials use of an ingoing wave boundary condition gives close agreement¹² with the optical-model phase shifts for the important range of L values. Both procedures will be employed. Even for forward angle scattering the cross section is not completely insensitive to this phenomenologically added absorption. Nevertheless it is possible to obtain information concerning the size of the nucleon wave function at the nuclear surface from the calculated tail of the potential.

Equation (5) differs from Eq. (4) in that to each partial wave with radial function $I_{L+\frac{1}{2}}(\alpha_s^{(0)} r')/(\alpha_s^{(0)} r')^{1/2}$ is added a small amount of the other solution, $K_{L+\frac{1}{2}}(\alpha_s^{(0)} r')/(\alpha_s^{(0)} r')^{1/2}$ irregular at the origin of the "receiver" nucleus, but finite elsewhere. Condition (B) ensures that logarithmic derivatives of the undistorted and distorted nucleon wave functions become nearly equal at the surface of the parent nucleus for large enough nuclear separation distances. A knowledge of the logarithmic derivatives of the nucleons' wave functions at this surface, determinable from their boundary energies, is all that is required and no specific nuclear model need be assumed. In region II the distorted wave functions for s and p waves are given by

$$\psi_{l,m} = \sum_L N_{L^l,m} u_{L^l}(r') Y_{L,m}(\theta', \varphi'). \quad (6)$$

In the above l stands for angular momentum with respect to the "parent" nucleus while L stands for angular momentum with respect to the "receiver" nucleus. The functions u_{L^l} are solutions of the radial equation,

$$\begin{aligned} (d^2/dr'^2)(r' u_{L^l}) \\ + \left\{ \frac{2m}{\hbar^2} [E_l^{(0)} - V] + \frac{L(L+1)}{r'^2} \right\} (r' u_{L^l}) = 0, \quad (7) \end{aligned}$$

obtained by numerical integrations performed with the aid of an IBM-709 computer. The $N_{L^l,m}$ are normaliza-

¹¹ An ingoing wave boundary condition has been used previously in heavy-ion calculations by R. L. Becker (unpublished) following the procedure used by H. Feshbach and V. Weisskopf, Phys. Rev. **76**, 1550 (1949) for the case of neutron-nucleus interaction.

¹² G. H. Rawitscher (to be published).

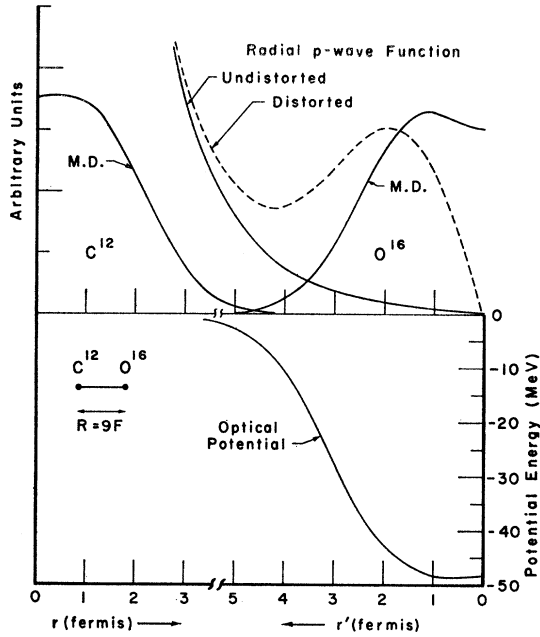


FIG. 1. Distortion of the radial wave function of a nucleon bound to C^{12} by an optical potential representing the nucleus of O^{16} . The distance from the center of C^{12} is measured by r ; r' is the distance from the center of O^{16} . For comparison the nuclear matter densities of the nuclei are also shown by the curves labeled M.D. in order to illustrate the very small matter overlap at a nucleus-nucleus distance of 9 F. The optical potential responsible for the distortion is shown in the lower half of the figures.

tion constants. The optical potential used has the form¹³

$$V = V_0 / \{1 + \exp[(r - R_0)/a]\} \quad (8a)$$

with extrapolated value V_0 lying between -50 and -60 MeV, and with

$$\begin{aligned} R_0 &= 1.25 \times A^{1/3} \text{ F}, \\ a &= 0.65 \text{ F}. \end{aligned} \quad (8b)$$

Matching the logarithmic derivative of the wave function in region II to that in region III fixes the value of the coefficient A_L as follows:

$$\begin{aligned} A_L^l &= -[I_{L+\frac{1}{2}}(\zeta_i)/K_{L+\frac{1}{2}}(\zeta_i)] \\ &\quad \times [\gamma_{L^l} - (d/d\zeta_i) \ln(I_{L+\frac{1}{2}}/\zeta_i^{l+1/2})] / \\ &\quad [\gamma_{L^l} - (d/d\zeta_i) \ln(K_{L+\frac{1}{2}}/\zeta_i^{l+1/2})], \end{aligned} \quad (9)$$

where

$$\begin{aligned} \zeta_i &= \alpha_i^{(0)} r' |_{r'=b}, \\ \gamma_{L^l} &= [1/\alpha_i^{(0)}] (d/dr') \ln u(r') |_{r'=b}. \end{aligned}$$

¹³ F. Bjorklund, in *Proceedings of the International Conference on the Nuclear Optical Model*, edited by A. E. S. Green, C. E. Porter and D. S. Saxon (Florida State University, Tallahassee, 1959), p. 1, slide 2. The imaginary part W_0 extrapolates to zero at zero nucleon energy and below. This of course implies in no way that there is no absorptive part of the nucleus-nucleus interaction. The spin orbit part of the potential is neglected in the calculation δE since its peak value at the nuclear surface is at most 15% of the value of the central potential. Hence its contribution to δE is nearly linear in $(l \cdot s)$ and become very small when averaged over the spins of the nucleons.

Despite the large size of the A_L^l , for values of R for which ΔE is calculated the ratios of $100 \times A_L \times K_{L+\frac{1}{2}} / I_{L+\frac{1}{2}}$ are always less than 6%. Values of the A_L^p are given in Table I for the cases of O^{16} scattering on C^{12} and of N^{14} on N^{14} . As noted previously, b is a distance from the center of the right nucleus beyond which the nucleon-nucleus potential is negligible. An example of a radial nucleon wave function u_0^1 which is a solution of Eq. (7) for the $C^{12}-O^{16}$ case with $l=1$, $L=0$, is shown in Fig. 1. For comparison the unperturbed wave function is also shown. Nuclear matter densities¹⁴ and the optical potential are shown in the same figure to illustrate the limitation on the region of applicability to this approach.

To facilitate the evaluation of the integrals in Eq. (2), Green's theorem and the Schrödinger equations for ψ and $\psi^{(0)}$ are used to transform the volume integral into surface integrals. This leads to the following expression for δE_i :

$$\delta E_i = \frac{-\langle \psi^{(0)*} \nabla \psi - \psi \nabla \psi^{(0)*} \rangle \cdot dS}{\int_{I+III} \psi^{(0)*} \psi d\mathbf{r}_i}, \quad (10)$$

where the integral in the numerator extends over the surface of region II which is taken as a sphere of radius a , while the volume integral in the denominator excludes region II. Hence setting the latter equal to 1 is a somewhat different approximation from the one originally stated in connection with Eq. (2b). The latter requires that

$$\int_{I+III} \psi^{(0)*} (\psi - \psi^{(0)}) d\mathbf{r} + \int_{II} \psi^{(0)*} (\psi - \psi^{(0)}) d\mathbf{r} \sim 0, \quad (11)$$

while in the former

$$\int_{I+III} \psi^{(0)*} (\psi - \psi^{(0)}) d\mathbf{r} - \int_{II} \psi^{(0)*} \psi^{(0)} d\mathbf{r} \sim 0. \quad (12)$$

If (11) is a good approximation (12) will be also since the identical first terms in the two expressions are small

TABLE I. Coefficients A_L^p for the $C^{12}-O^{16}$ interaction, calculated using a (real) Woods-Saxon potential [Eq. (8a)] with parameters $V_0 = -50$ MeV, $a = 0.650$ F, $R = 1.25 A^{1/3}$ F.

L	A_L^p (15.6-MeV neutron)	A_L^p (18.7-MeV neutron)
0	473.7	204.78
1	623.3	310.94
2	150.9	57.28
3	31.19	12.17
4	7.19	2.03
5	1.09	0.26

¹⁴ H. F. Ehrenberg and R. Hofstadter, *Phys. Rev.* **113**, 666 (1959), Eq. (A).

if $\psi - \psi^{(0)}$ is small in regions I and III, i.e., everywhere but in the second nucleus; while the smallness of the nonidentical second terms depends on the same circumstance, namely, the smallness of $\psi^{(0)}$ in region II. Substitution of Eq. (5) into Eq. (10) leads to the following expression for the s -state nucleons:

$$\delta E_s = -(\hbar^2/2m)[c_s c_s^{(0)}/\alpha_s^{(0)}] \sum_{L=0}^{\infty} A_L^s [\xi_L^s(\alpha_s^{(0)} R)]^2, \quad (13)$$

where c_s and $c_s^{(0)}$ are as in Eqs. (3) and (5), respectively. The corresponding expressions for three p -state nucleons, summed over the three values of m lead to

$$3\delta E_p = -(\hbar^2/2m)[3c_p c_p^{(0)}/\alpha_p^{(0)}] \times \sum_{L=0}^{\infty} A_L^p \left\{ \sum_{m=-1}^{+1} [\xi_L^{p,m}(\alpha_p^{(0)} R)]^2 \right\}, \quad (14)$$

where c_p and $c_p^{(0)}$ are the quantities which occur in Eqs. (3) and (5). To obtain the long-distance part of the nucleus-nucleus potential energy function the contributions from Eqs. (13) and (14) are summed over the nucleons whose wave function tails originate in region I. To this is added a similar contribution obtained by interchanging the roles of two nuclei, the one which formerly had served as a potential field for the nucleon wave function tails (region II) now assuming the role of a nucleus from which the tails of the wave functions of individual nucleons are pictured as protruding (region I). The other nucleus which had formerly served as the source of the nucleon wave function tails now assumes the role of an optical potential field. Higher order corrections in which, for example, the optical potential is modified by the distance of the nucleus in region II caused by the "tails" from region I, are neglected.

Strictly speaking the above procedure applies only to neutrons. However, as an approximation, in the summation over nucleons the proton contributions are taken equal to those of the corresponding neutrons because for the nuclei here considered, C^{12} , O^{16} , and N^{14} , the reduction of the size of the proton wave function in region II due to the added repulsion of the ~ 2 -MeV Coulomb barriers is compensated to some extent by enhancement of this wave function in region II due to the decrease of about 2 MeV in the binding energy of protons compared to the corresponding binding energy of neutrons for these nuclei. However as discussed in Breit and Ebel¹⁵ for $N^{14}-N^{14}$ tunneling, the enhancement appears to overcompensate the reduction.

The resulting expression for $\Delta E(R)$ is used in the next section as a two-body potential-energy function to approximate the nucleus-nucleus interaction for sufficiently large values of R . It still contains the undetermined constants $c_p^{(0)}$, c_p for each of the two nuclei which

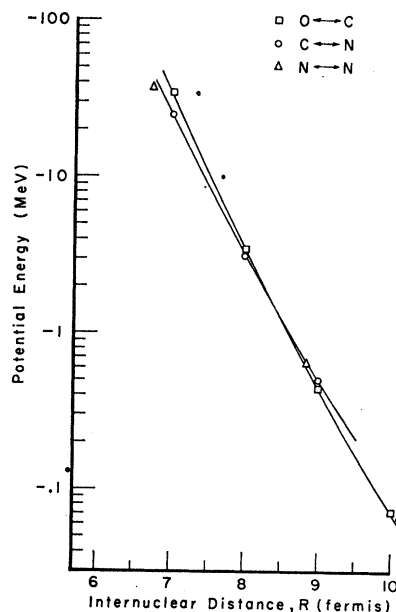


FIG. 2. Calculated nucleus-nucleus ΔE potentials using the single-particle reduced-width parameters ρ_{sb} given in Table III. These curves must be multiplied by factors of 0.16, 0.14, and 0.17 for the O-C, C-N, and N-N systems, respectively, so as to obtain near agreement with experiment, as described in the text.

are proportional to the single particle reduced widths described in Sec. III. The value of this constant is adjusted to fit experiment and the reduced width is thereby determined. Examples of the potentials so determined for the systems $C^{12}-O^{16}$, $C^{12}-N^{14}$, and $N^{14}-N^{14}$ are illustrated in Fig. 2.

For small internuclear separation distances R the method of calculation of the interaction between the two nuclei cannot be expected to be valid since the nuclei are significantly deformed by one another's presence, each nucleus may become excited either actually or virtually, etc. Fortunately the elastic scattering cross section is not very sensitive to the exact R dependence of the real part of the potential for small values of R , e.g., for values of R less than that at which the real part of the Coulomb plus nuclear potential vanishes, so long as there is sufficient absorption. By absorption is meant any process which removes particles from the elastic scattering beam. These processes cause the nuclear phase shifts K_L to become complex,

$$K_L = a_L + ib_L,$$

with a_L and b_L both real. An attempt at a full solution of the problem with the allowance for the opening of many channels is of course not practical; so the effects of the inelastic and reactions processes may be simulated in the usual ways, either by the addition of a complex part to the potential energy or by the imposition of a boundary condition.^{11,12} Both methods have been employed in this work. The effect of either procedure,

¹⁵ G. Breit and M. E. Ebel, Phys. Rev. **103**, 700 (1956).

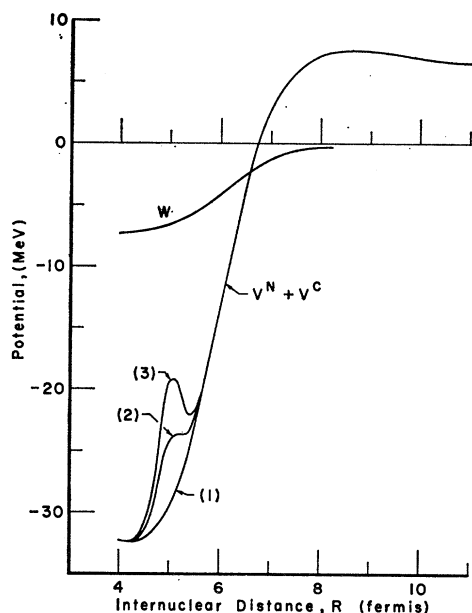


FIG. 3. Arbitrary modifications of a real nuclear plus Coulomb potential $V^N + V^C$ introduced in order to investigate the sensitivity of the cross sections to the value of the potentials in the region where the modifications were made. To the potential curve (1) Gaussian-shaped "bumps" of magnitudes 5 and 10 MeV have been added as shown in curves 2 and 3, respectively. For comparison the imaginary part of the potential, W , is also shown. Results for phase shifts are shown in Table III.

when compared to the results obtained in the absence of absorption, is to shift the angular positions of the maxima and minima of the ratios of the cross section to the Coulomb cross section and in addition to reduce greatly the amplitudes of the peaks and valleys in the angular distribution curve.

For convenience in calculation, the ΔE potential has been arbitrarily rounded off for internuclear separation of less than about 6 F and the resulting potential is denoted by $\mathcal{U}(R)$. For amounts of absorption necessary to give fits to the experiment under consideration large modifications in the real part of the potential inside this distance produce little change in phase shifts. Although it is difficult to formulate the effect precisely an example may serve to illustrate the point. Figure 3 shows a plot of a typical ΔE plus Coulomb potential for $N^{14}-N^{14}$ scattering, but not the one with the properly adjusted c_p . The R dependence of \mathcal{U} is either the one suggested by Woods-Saxon

$$\mathcal{U}(R) = \mathcal{U}_0 / [1 + \exp(R - \mathcal{R})/a], \quad (15a)$$

with a determined by the calculated value of $\Delta E(R)$ and \mathcal{R} so adjusted that the rounding off of the potential is negligible beyond 6 F, or else

$$\mathcal{U}(R) = \mathcal{U}_0' \exp(-R/a) \quad (15b)$$

is also used in connection with the ingoing wave boundary (IWB) procedure. Curve (1) exhibits a typical

rounding off and in curves (2) and (3) modifications have been arbitrarily added to this potential inside 6 F. The modifications are "bumps" with Gaussian shapes, of width 2 F and magnitudes 5 and 10 MeV, respectively. On the same figure is plotted the empirical imaginary part of the potential W . In Table II are shown the effects of the added potential "bumps" on $\exp(-2b_L)$, $\exp(-2b_L) \sin 2a_L$, combinations of the real and imaginary parts of the phase shift used directly in the cross-section calculation at 12 MeV. The agreement between the three sets of values is typical of those for $N^{14}-N^{14}$ and $C^{12}-N^{14}$ scattering at the energy under consideration, and the differential cross sections computed from the three are almost indistinguishable. This is understandable for the case in which the absorption is strong and takes place mostly inside the Coulomb + centrifugal + nuclear barrier. For the smaller L waves, the real phase shifts a_L are modified by a change in the potential, but these waves are in any case strongly absorbed and the cross section is little changed. For the higher partial waves the values of $\mathcal{F}_L(R)$, where $\mathcal{F}_L(R)$ is a solution finite at the origin of the radial equation

$$\frac{d^2 \mathcal{F}_L}{dR^2} + \left\{ \frac{2\mu}{\hbar^2} [E - \mathcal{U}(R)] - \frac{L(L+1)}{R^2} \right\} \mathcal{F}_L(R) = 0, \quad (16)$$

are small because of the centrifugal barrier in the region of the added hump. Thus the phase shifts are little modified. Likewise, changes in the shape of W , so long as (a) W is large at distances smaller than the barrier region and (b) the tail of W does not extend significantly into this region, have been found to produce little change in the cross section. Typical examples of various W 's are shown in Fig. 4 and the resulting ratios of the cross sections to Rutherford in Fig. 5.

TABLE II. Effect of potential changes on phase shifts. The nuclear phase shifts are denoted by $K_L = a_L + ib_L$. The numbers in parentheses refer to the potential curves shown in Fig. 3. The results labeled IWB are obtained from the potential curve (2) and the imposition of the ingoing wave boundary condition on the wave function at $R=4$ F, as described in the text. The table illustrates that the introduction of potential "bumps" at distances less than 6 F does not appreciably affect the phase shifts and or cross sections.

L	IWB	$\exp(-2b_L)$			$\exp(-2b_L) \sin 2a_L$			
		(1)	(2)	(3)	IWB	(1)	(2)	(3)
0	0.087	0.090	0.098	0.109	-0.079	-0.090	-0.098	-0.108
1	0.093	0.070	0.078	0.093	-0.080	-0.070	-0.076	-0.087
2	0.106	0.106	0.115	0.129	-0.080	-0.096	-0.104	-0.114
3	0.128	0.102	0.111	0.126	-0.074	-0.083	-0.084	-0.090
4	0.164	0.156	0.169	0.184	-0.055	-0.071	-0.077	-0.088
5	0.220	0.192	0.201	0.214	-0.015	-0.045	-0.044	-0.047
6	0.307	0.295	0.307	0.320	0.049	0.043	0.037	0.025
7	0.440	0.427	0.430	0.431	0.138	0.114	0.107	0.098
8	0.626	0.630	0.630	0.627	0.223	0.216	0.208	0.197
9	0.826	0.822	0.818	0.811	0.235	0.204	0.202	0.201
10	0.951	0.938	0.938	0.937	0.153	0.136	0.136	0.173
11	0.991	0.982	0.981	0.982	0.072	0.066	0.066	0.067
12	0.999	0.995	0.994	0.994	0.030	0.029	0.029	0.029
13	1.000	0.998	0.998	0.998	0.012	0.012	0.012	0.012

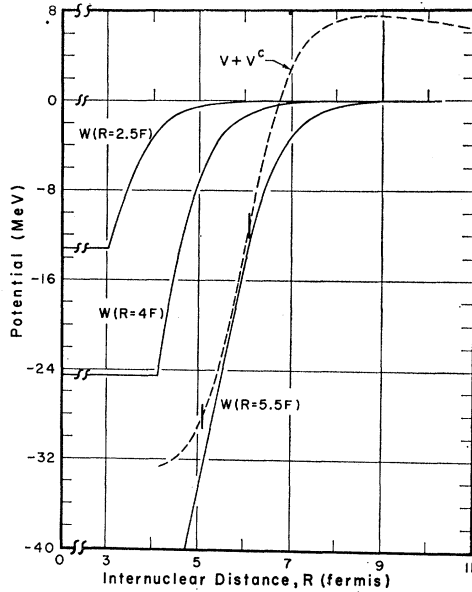


FIG. 4. Plots of various imaginary potentials W used to demonstrate the insensitivity of the cross section to W . The explanation for the parametrization of W as a function of r is given in Fig. 5, which also shows the resulting cross sections.

As an alternative to the addition of a complex part to the potential, absorption inside a given value of R , say $R_b \sim 1.2 F$ ($A_1^{1/3} + A_2^{1/3}$), may be obtained by using for each L a one-dimensional boundary condition imposed at R_b . If it is assumed that a two-body nuclear potential is valid at least down to R_b and if R_b is far enough inside of the barrier formed by the nuclear, Coulomb and centrifugal potentials—henceforth called simply barrier—so that the JWKB approximation becomes valid for the significant values of L and if the outgoing branch of the JWKB expression for the wave function is set equal to zero,¹² then the radial wave functions are given by

$$\mathfrak{F}_L(R) = k_L(R)^{-1/2} \exp \left[-i \int^R k_L(r) dr \right];$$

$$k_L(r) \equiv \left\{ \frac{2\mu}{\hbar^2} [E - \mathcal{V}(r)] - \frac{L(L+1)}{r^2} \right\}^{+1/2}. \quad (17)$$

In this case the resulting phase shifts are uniquely determined and are independent of the value of the nuclear potential for $r < R_b$. The nuclear wave functions are then obtained by imposing at R_b the IWB boundary condition

$$(d\mathfrak{F}_L/dR)/\mathfrak{F}_L = \left[-\frac{1}{2} (dk_L/dR)/k_L - ik_L \right]_{r=R_b}$$

and the resulting phase shifts lead to essentially the same scattering cross sections¹² as a certain class of potentials the real parts of which vary widely inside R_0 . Use of the IWB has the advantage of exhibiting the fact that for strong enough absorption several arbitrary

parameters introduced into W and in rounding off V are superfluous and that in reality the only empirically added parameter to which the results are sensitive is one of the reduced width type, ρ , defined below. This of course implies the validity of the ΔE potential in the barrier region. The value of R_b is chosen sufficiently small to be well inside the barrier so that the JWKB approximation is valid. The largest values of R_b where this is true were found to be between 1.20 F and 1.25 F times $A_1^{1/3} + A_2^{1/3}$ at which point some many-body features probably still persist and the calculated two-body potential is therefore probably not valid. Since the high L contributions to the cross section do not depend strongly on the close-in interaction and the low L contributions are small on account of the large effect of absorption, it is the 3 or 4 intermediate L contributions whose validity is most questionable in the calculations reported on in this paper. Strictly speaking either the procedure of using a complex potential or of describing its effect by the IWB method may be looked on as calculational methods of obtaining values of the quantities $\exp(-2b_L)$, $\exp(-2b_L) \sin 2a_L$ which vary smoothly with L in such a way as to describe the experimental facts.

The considerations following Eq. (12) of Sec. II show that the nucleus-nucleus potential is formed from a sum of terms each of which is proportional to the product of the constants $c_p^{(0)}$ and c_p which furnish the unknown values of the nuclear wave functions at the nuclear sur-

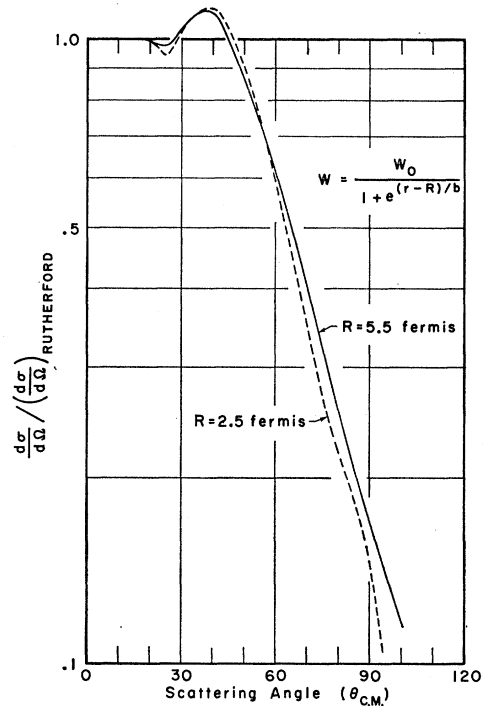


FIG. 5. Sensitivity of the cross section to the imaginary potential W .

face. In principle each p -wave nucleon has a separate $c_p^{(0)}$ and c_p . In view of the crudeness of some of the aspects of the theory it was not felt warranted to treat the $p_{1/2}$ nucleons differently from the $p_{3/2}$ nucleons in all cases even though appreciable differences exist occasionally. However in O^{16} , for example, the binding energy of a $p_{3/2}$ nucleon as determined from the $p-p'$ inelastic scattering experiments¹⁶ is approximately 23 MeV which is considerably larger than the separation energy of the $p_{1/2}$ nucleon which is 15.6 MeV. In order to evaluate the effect on ΔE due to this relatively large difference in separation energies a sample calculation was done in which it was found that the contribution to ΔE of three p neutrons bound at 23 MeV is roughly half of the corresponding quantity for neutrons bound at 15.6 MeV for R between 7 and 8 F. Therefore, it was felt that eight p nucleons bound with 15.6 MeV would be reasonably equivalent to the four $p_{1/2}$ nucleons + eight $p_{3/2}$ nucleons, and the calculations have been so carried out. In the cases of C^{12} and N^{14} , the contribution to ΔE of four s nucleons were neglected because of their large separation energy and the rest of the nucleons were treated as having the same separation energy of 18.7 and 10.54 MeV, respectively.

The contribution of the s nucleons was neglected altogether since their number is less than half of the number of p nucleons for all the nuclei here considered and, from the above $p_{3/2}-p_{1/2}$ comparison, their contribution to ΔE should be less than a 20% of the total value. Consequently two unknown parameters remain, one for each of the two heavy nuclei. These are denoted by ρ and ρ' and are given by

$$\begin{aligned}\rho &= c_p^{(0)} c_p, \\ \rho' &= c_p^{(0)'} c_p'.\end{aligned}\quad (18)$$

The value of \mathcal{U}_0 of Eq. (15a) is first determined so as to give the best fit between the experimental¹⁷ and theoretical nucleus-nucleus scattering cross sections, and then, from the knowledge of the R dependence of the δE_p 's, a relation involving ρ and ρ' is obtained. By considering the system $N^{14}-N^{14}$, $\rho = \rho' = \rho(N^{14})$ can be determined. From this value and the knowledge of \mathcal{U}_0 for the $N^{14}-C^{12}$ system, $\rho(C^{12})$ can in turn be obtained, and the results are contained in Table III.

The parameter ρ is directly proportional to the average reduced widths of the bound nucleons. It is convenient to express it in terms of a fictitious "single-particle" quantity ρ_{sb} , which is obtained by considering the wave function of a single-particle bound to a real

TABLE III. Ratio of reduced width parameter ρ to single-body parameter ρ_{sb} . The latter is calculated from the potential given in Eq. (19).

Nucleus	ρ_{sb}	ρ/ρ_{sb}
C^{12}	48.0 F ⁻³	0.15
N^{14}	6.9	0.17
O^{16}	41.0	0.16

potential well of a Woods-Saxon type

$$V^m = V_0^m \{1 + \exp[(r - 1.2(A - 1)^{1/3} F)/0.50 F]\}^{-1}. \quad (19)$$

The value of V_0^m is determined by demanding that the p nucleon be bound at the experimentally observed separation energy, and from the knowledge of the normalized wave function, $c_{sb}^{(0)}$ can be determined. The square of the absolute values of the s and p wave functions bound by this well can then be used to determine a nuclear density, and comparison with the charge densities determined from electron scattering¹⁴ shows reasonable agreement, as illustrated in Fig. 6.

In Table III the values of ρ as well as of ρ/ρ_{sb} , as determined by the procedure described above, are shown for C^{12} , N^{14} , and O^{16} . The choice of $c_{sb}^{(0)}$ and hence the value of ρ/ρ_{sb} is dependent upon the model assumed for the undistorted nuclei. For the N^{14} nucleus, a square well of radius 3.22 F and depth 35 MeV binds a p nucleon at -10 MeV, and the value of $c_{sb}^{(0)}$ is $2.35 F^{-3/2}$, which is to be compared with a value of $2.63 F^{-3/2}$ obtained when the square well is replaced by a Woods-Saxon well. These potential wells are chosen so that the resulting charge distributions approximate those obtained from electron scattering experiments¹⁴ as shown on Fig. 6, in whose figure caption the explicit form of the charge density obtained from electron scattering is given, and are not the same as the nucleon-nucleus optical potentials used above. The matter distribution derived from the s and p nucleons bound by the square well fit the experimental charge distribution reasonably well. If the radius of the square well is changed to 3.5 F, and the depth chosen so that a p nucleon is bound at the same -10 MeV, then the corresponding value of $c_{sb}^{(0)}$ is $2.97 F^{-3/2}$ but the matter distribution no longer approximates the experimental one as well, as is also illustrated in Fig. 6. The three potentials mentioned in the examples above lead to values of ρ_{sb} which differ from each other by about 50% or less. The value of $(\rho/\rho_{sb})_{O^{16}}$ is not well determined since the procedure used in this paper does not reproduce the wiggle in the cross sections, although giving a good over-all fit. It may be noted that ρ/ρ_{sb} appears to vary less with atomic weight A than does ρ itself. If the value of c_p is assumed equal to $c_p^{(0)}$, then $c_p^{(0)}$ can be obtained as the square root of ρ given in the table, and the corresponding value of the nucleon wave function beyond the nuclear "surface" is given by Eq. (3). A value for the usual reduced width parameter γ^2 can

¹⁶ H. Tyren, P. Hillman, and Th. A. J. Maris, Nucl. Phys. 7, 10 (1958).

¹⁷ J. A. Kuehner and E. Almqvist, Bull. Am. Phys. Soc. 6, 48 (1961). The authors are very grateful to Dr. Almqvist for providing supplementary unpublished data for $N^{14}-C^{12}$ and $O^{16}-C^{12}$ scattering. Their results differ somewhat from the earlier data reported by M. L. Halbert, C. E. Hunting, and A. Zucker, Phys. Rev. 117, 1545 (1960), also shown in Fig. 6.

thus be obtained. For N^{14} , if the nuclear radius b is taken equal to 3.22 F, then¹⁸ $\gamma^2 = \mathcal{F}^2 / (2m/\hbar^2) \sim 1.15$ MeV F. This quantity, when expressed in units of $3\hbar^2 / (2 \text{ mb})$, is equal to 0.12, which of course depends on the choice of b . A source of error in the determination of the value of ρ is due to the uncertainty in the theoretical value of ΔE . This uncertainty increases with decreasing internuclear separation, as the distortion and matter overlap between the two nuclei increases. At 8 F, which is the distance for which the sum of nuclear plus Coulomb potentials, as used in the fits to experiments, reaches a broad maximum, the overlap integral of the distorted and undistorted nucleon wave function, $(\psi^{(0)}, \psi)$, differs approximately by 20% from unity for the three nucleus-nucleus systems investigated. For this estimate the value of ρ is assumed identical to ρ_{sb} , and $\psi^{(0)}$ is assumed equal to the expression given in Eq. (3) for all values of r . Since $\rho < \rho_{sb}$, this overlap estimate is considerably too large perhaps by a factor of ≈ 2 but it nevertheless serves as an indication for the theoretical uncertainty in ΔE due to wave function distortion effects not taken into account. At that distance the overlap of the matter density of the two nuclei, if assumed undistorted, is less than 1%. In order to investigate the sensitivity of ρ to the uncertainty in ΔE , various arbitrary modifications of the nuclear potential in the barrier region were performed. For example, various smooth changes in ΔE which produce 10% modifications in ΔE at distances of 2 F, 1.4 F, and 0.6 F to the left of the top of the barrier, which in this example is at 8.6 F, result in changes of 3, 8, and 33%,

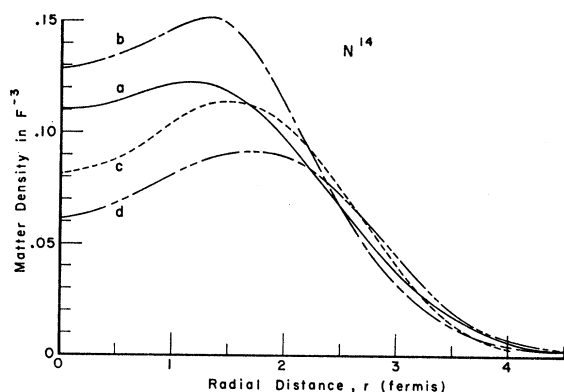


FIG. 6. Matter densities for N^{14} for various choices of the auxiliary potential V^M , Eq. (19). Curve a represents the charge density obtained from electron scattering experiments,¹⁴ given by $\rho = [(1 + r^2/a_0^2) \exp(-r^2/a_0^2)] / [\pi^{1/2} a_0^3 (2 + 3\alpha)]$ with $a_0 = 1.8$ F and $\alpha_H = 5/3$. Matter densities computed from s and p nucleon wave functions corresponding to the Woods-Saxon potential, Eq. (19), and to square-well potentials with radii 3.22 and 3.50 F are given by curves b, c, and d, respectively. The depths of all potentials are chosen so that a p nucleon is bound with an energy of -10 MeV. The densities of two s -wave nucleons are averaged with those of seven p -wave nucleons. The values of ρ_{sb} corresponding to curves b, c, and d are 6.9, 5.5, and 8.8 F^{-3} , respectively.

¹⁸ G. Breit, in *Handbuch der Physik*, edited by S. Flügge (Springer-Verlag, Berlin, 1959), Vol. 41, Part 1, Sec. 33.

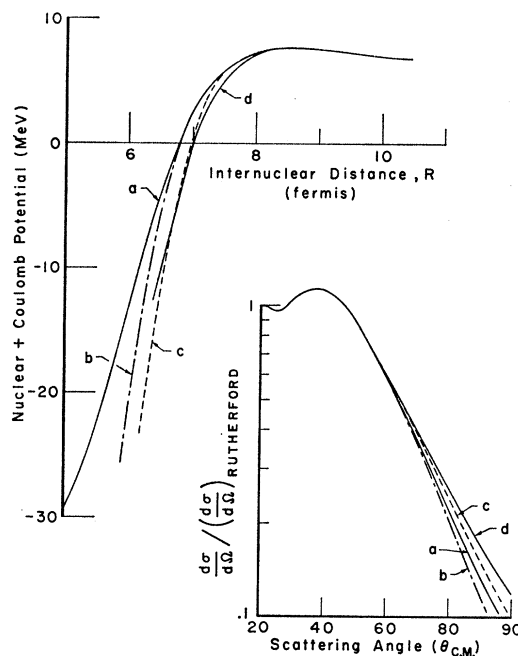


FIG. 7. Sensitivity of cross section to modifications of the potential in the "barrier region." The curves b, c, and d join curve a smoothly at 7 F, 7.5 F, and 8 F, respectively. The potential marked a is the same as potential (1) in Fig. 3. The corresponding cross sections are shown in the insert. The IWB condition was used in all the calculations at approximately 5 F. The difference between cross sections a and b is apparently due to difference of the steepness of the two potentials. The similarity of the cross sections at angles less than 60° is presumably connected to the fact that all potentials have the same maximum at about 8.5 F.

respectively, of the cross section at an angle where the cross section is nearly $\frac{1}{4}$ of the Coulomb cross-section value. These results are illustrated in Fig. 7. These changes would lead, respectively, to changes in ρ by factors of roughly 1.2, 1.5, and 3. It is therefore believed that an uncertainty estimate in ρ of a factor 2 is conservative.

Comparison between theoretical and experimental¹⁷ cross sections is shown in Fig. 8. The over-all fit to experiment is reasonable, although small oscillations are not reproduced in detail. These may well be due to features in the interactions not accounted for by the somewhat rough assumptions made in this work. For example, if resonances for particular L waves should occur,¹⁹ phase shifts derived from two-body potentials may prove insufficient for the description of experiments. Indeed as mentioned above reasonable fits to experimental data¹⁷ for $C^{12}-O^{16}$ scattering at 8-, 9-, and 10-MeV center-of-mass energies are obtainable with the procedure outlined above employing the same potential in all three cases. At 11.57 and 13.67 MeV, fits are not possible indicating that some more complicated feature has entered.

¹⁹ D. A. Bromley, J. A. Kuehner, and E. Almqvist, *Phys. Rev.* **123**, 878 (1961).

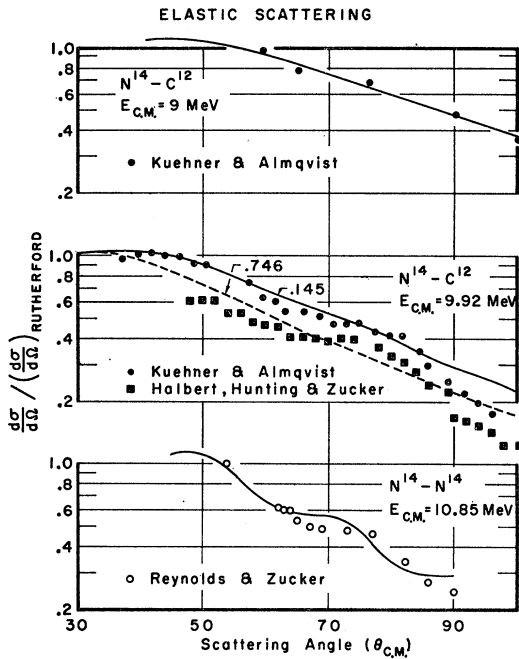


FIG. 8. Comparison of theoretical with experimental angular distributions. The fits are obtained by varying the parameter ν_0 given in Eq. (15a), as explained in the text. σ in Eq. (15a) is not a "significant" parameter and α is obtained from theoretical considerations. The values listed in Table III are obtained from the best fits, shown here. The numbers indicated for the two 9.92 MeV $N^{14}-C^{12}$ curves indicate the factors by which the ΔE potential shown in Fig. 2 must be multiplied so as to obtain the corresponding cross sections.

Finally, it may be noted that even at the high energies, where the assumptions made in the theoretical treatment outlined above are not expected to be valid, a reasonable agreement with experimental $O^{16}-C^{12}$ and $C^{12}-N^{14}$ cross sections^{20,21} is obtained, as shown in Fig. 9. The reduced width parameters employed in these comparisons are the same as those used for the low-energy fits, and are given in Table III.

In Fig. 10 the absolute value of the potentials used is plotted against the nucleus-nucleus distance R . The curve labeled ΔE corresponds to an average of the potentials shown in Fig. 2, calculated employing single-particle reduced widths. The curve marked " $\Delta E/5$ " represents an average of the potentials used in fitting the experimental cross sections, as shown in Figs. 8 and 9. The ratio of potentials at the same R for the two curves is approximately $\frac{1}{5}$. The exact value of this ratio is ρ/ρ_{sb} of Table III. The curve labeled Ov represents the overlap integral

$$\int \rho_1(\mathbf{r}-\mathbf{R})V_2(\mathbf{r})d\mathbf{r} = V_{12}(\mathbf{R}) \quad (20)$$

evaluated for the $N^{14}-N^{14}$ collision. Here $\rho_1(\mathbf{r}_1)$ is the

²⁰ D. J. Williams and F. E. Steigert, Nucl. Phys. **30**, 373 (1962).

²¹ A. M. Smith and F. E. Steigert, Phys. Rev. **125**, 988 (1962).

matter density of the first nucleus at a point displaced by vector \mathbf{r}_1 from the center of nucleus 1. The displacement vector from the center of the second nucleus to the center of the first is denoted by \mathbf{R} and the vector from the center of the second nucleus to a point P by \mathbf{r} . The optical-model potential of a nucleon at point P exposed to the field of the second nucleus is designated by $V_2(\mathbf{r})$.

On the most naive interpretation of the nucleon-nucleus optical-model potential the integrand of Eq. (20) is the potential energy of the nucleons belonging to the first nucleus caused by their interaction with the second nucleus. It is realized that both $\rho_1(\mathbf{r}-\mathbf{R})$ and $V_2(\mathbf{r})$ are affected by the proximity of the nuclei to each other, that $V_2(\mathbf{r})$ has not been shown to have the simple meaning given to it in Eq. (20) and that the velocity dependence of V_2 is neglected. In addition to the neglect of these and other effects having their origin in the mathematical difficulties of the many body problem and the incompleteness of information regarding nucleon-nucleon interactions the value of ρ_1 for large values of $|\mathbf{r}-\mathbf{R}|$, i.e., in the "tail" of the matter-density distribution curve, is not believed to be known with certainty, the main emphasis in the Stanford fits¹⁴ to electron-nucleus scattering data being in obtaining the general shape of the ρ_1 versus distance curve. The precise values obtained from Eq. (20) may thus be

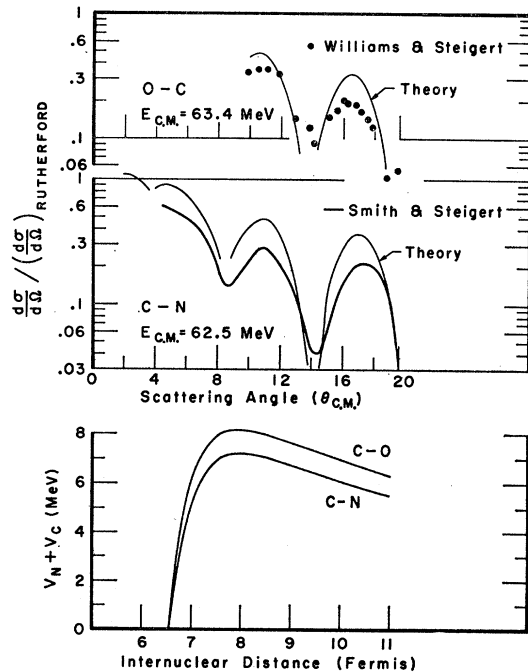


FIG. 9. Comparison of theoretical cross sections with experiment. The parameters employed in the theory are the same as those used for the low-energy results shown in Fig. 8 and listed in Table III. The experiments for $O^{16}-C^{12}$ and $C^{12}-N^{14}$ are those of Refs. 20 and 21, respectively. The lower part of the figure illustrates the sum of nuclear and Coulomb potentials employed in the calculation of the cross sections.

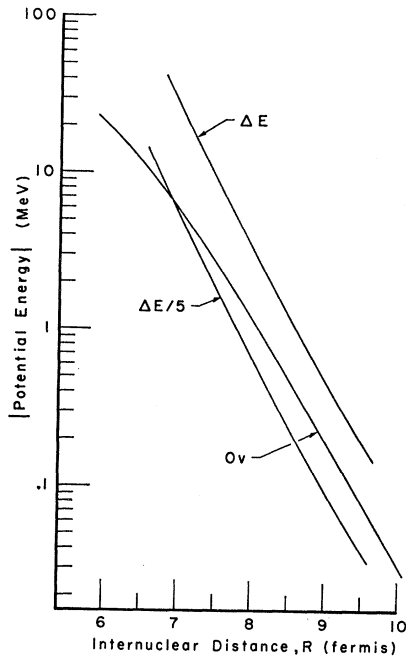


FIG. 10. Summary of nucleus-nucleus potentials. The top curve labeled ΔE is an average of the theoretical potential for the $C^{12}-O^{16}$, $C^{12}-N^{14}$, and $N^{14}-N^{14}$ systems, for which single-particle reduced-widths are employed. The individual potentials are shown in Fig. 2. The curve labeled Ov represents an overlap integral of matter density and nucleon-nucleus optical potential, as described in the text, and the lower curve is an approximate representation of the nuclear potentials calculated for the reduced widths as required from the comparison with the experimental scattering cross sections.

subject to question. It is nevertheless striking that the curve Ov obtained in this manner is not in very decided disagreement with the curve marked $\Delta E/5$ in Fig. 10, the agreement being good at 7 F and a discrepancy by a factor of only about 2 developing at 9.5 F. It may be remarked that within the approximations used here

$$V_{12}(\mathbf{R}) = \int \rho_2(\mathbf{r}) V_1(\mathbf{r}-\mathbf{R}) d\mathbf{r} \quad (20')$$

is an alternative form of the potential energy between nuclei 1 and 2. On account of the identity of the two nuclei involved there is no difference between (20) and (20') in this case.

CONCLUSIONS

From this study of the scattering of heavy nuclei by heavy nuclei the following conclusions may be drawn:

(1) That although the forward-angle elastic scattering is not completely determined by the tail of the potential calculated from nucleon-nucleus data, if sufficient absorption from the incident beam is allowed for, then the tail of the potential strongly affects the angular distribution and agreement with the over-all shape of the experimental angular distribution curve is obtained, even though the wiggles may not be reproduced in detail.

(2) That the tail of the potential calculated from the binding-energy consideration outlined in Sec. II is well enough determined by the experimental data on elastic scattering to lead to a rough value of the reduced width which is of the order of one- or two-tenths the single-particle value.

The above outlined procedure would appear to be a reasonable starting point for further, more detailed, calculations taking into account spins, nuclear deformation, Coulomb excitation, nuclear excitation, etc.

ACKNOWLEDGMENTS

The authors wish to gratefully acknowledge the suggestion by Professor G. Breit of calculating the tail of the nucleus-nucleus potential from the nucleon-nucleus potential and for numerous discussions on all phases of the work. They also wish to acknowledge the help of Professor R. L. Gluckstern for suggestions relating to numerical work in the integration of the radial wave equation, of Dr. G. Herling for use of his machine program from which some of the Coulomb functions were obtained in the early stages of the work, and of Dr. D. J. Williams, V. H. Mesch, and particularly of J. Polak for help received in machine computations.